IEEE Access
Multidisciplinary | Rapid Review | Open Access Journal

Received December 13, 2018, accepted January 8, 2019, date of publication January 17, 2019, date of current version February 6, 2019.

Digital Object Identifier 10.1109/ACCESS.2019.2892812

Adaptive Downlink OFDMA System With Low-Overhead and Limited Feedback in Time-Varying Underwater Acoustic Channel

GANG QIAO[1,2,3], (Member, IEEE), LEI LIU[1,2,3], LU MA[1,2,3], (Member, IEEE), AND YANLING YIN[4], (Member, IEEE)

[1]Acoustic Science and Technology Laboratory, Harbin Engineering University, Harbin 150001, China
[2]Key Laboratory of Marine Information Acquisition and Security, Ministry of Industry and Information Technology, Harbin Engineering University, Harbin 150001, China
[3]College of Underwater Acoustic Engineering, Harbin Engineering University, Harbin 150001, China
[4]College of Electrical and Information, Northeast Agricultural University, Harbin 150030, China

Corresponding author: Lu Ma (malu@hrbeu.edu.cn)

This work was supported by the National Natural Science Foundation of China under Grant 61431004, Grant 61601136, and Grant 61601137.

ABSTRACT Because of the time-varying characteristic and the large propagation delay in underwater acoustic (UWA) channel, adaptive resource allocation in UWA orthogonal frequency-division multiplexing access (OFDMA) system cannot be performed with the assumption of perfect channel state information (CSI) at the transmitter. Therefore, this paper focuses on the outdated CSI and proposes an adaptive downlink OFDMA system with low-overhead and limited feedback in time-varying UWA channel. First, a data fitting method is proposed for channel reconstruction, which shows better performance and lower overhead than the traditional group quantization method in simulations. Second, we define the per-subcarrier channel temporal correlation (PSCTC) and long-term statistical mean value as two indicators of outdated CSI, for optimizing CSI feedback in UWA channel with large propagation delay. Finally, a CSI selection method based on channel correlation attenuation (CCA) factor is proposed, where CSI used for feedback is selected between outdated-instantaneous CSI and outdated-average CSI according to the CCA factor in the current observation period. Sea trail results show that the CSI reconstruction based on data fitting method has lower bit error ratio and less overhead than traditional group quantization method. The PSCTC coefficient is related to the feedback delay, and the long-term statistics is stationary, which means that the outdated-average CSI is suitable for channel feedback. The CSI selection method based on CCA factor has better performance than that only uses outdated-instantaneous CSI or outdated-average CSI under different time-varying channel conditions in experimental results.

INDEX TERMS UWA communications, OFDMA, outdated CSI, long-term statistics, data fitting, CCA.

I. INTRODUCTION

Multicarrier modulation in the form of orthogonal frequency division multiplexing (OFDM) is the main choice for recent broadband wireless systems, including WiFi, WiMax, and 4G cellular systems. The multiuser extension, orthogonal frequency-division multiple access (OFDMA), allows multiple users to transmit data on different subcarriers at the same time. The study on multiuser OFDM is extensive in the context of broadband terrestrial communication systems, see e.g., [1]–[5], and references therein.

The research development in the underwater domain lags far behind that in the radio world, partly because the underwater environment is more challenging, the experimental operations are costly, and the research community is much smaller. Only in recent years, significant progress has been made on the adoption of OFDM as a viable option for point-to-point UWA communications [6]–[12], and OFDM based multiple access (OFDMA) is also used in UWA communication networks [13]–[17]. OFDMA retains the high frequency band utilization characteristics of OFDM, and uses the

orthogonality of the carriers in OFDM to achieve collision-free multiple access. It can also provide flexible spectrum access through adaptive technology, so that each user is able to avoid the deep fading subcarriers, and obtains multi-user gain in parallel access.

Because of the time-varying, space-variant and frequency-varying characteristics in UWA channel, UWA communication systems often use the most conservative modulation parameters to satisfy the worst channel state, leading to a big loss in spectral efficiencies. Therefore the adaptive modulation technologies have received attention for both point-to-point UWA communications [18]–[21] and multi-user cases [14], [22], [23] in recent years.

Rice *et al.* [24] proposed an adaptive transmit power control transmission scheme for UWA communication systems. Benson *et al.* [25] designed an adaptive modulation scheme to select the best technique for a given UWA channel between coherent modulation (phase-shift keying (PSK) and quadrature amplitude modulation (QAM)) and noncoherent (multiple frequency shift keying (MFSK)) modulation. Mani [26] studied the adaptive modulation and coding technology under PSK modulation, mainly considering the constellation size of multi-band phase shift keying (binary PSK (BPSK), quadrature PSK (QPSK), 8PSK) and the performance of Turbo codes at different bit rates under variable transmission rates. At present, scholars start to focus on UWA adaptive OFDM systems. An adaptive OFDM system to maximize the throughput under a target average BER was proposed by Radosevic *et al.* [19], where the CSI is sent back to the transmitter by a radio link, and the adaptation depends on the one data packet ahead channel prediction, and the modulation modes include BPSK, QPSK, 8PSK and 16QAM. An adaptive modulation and coding (AMC) system based on effective SNR(ESNR) was proposed by Wan *et al.* in 2014 [21], in the experiment, the ESNR is transmitted and fed back by an acoustic link to select a finite number of transmission modes in underwater OFDM. Compared with the traditional pilot SNR (PSNR) in OFDM, the proposed ESNR considers the estimation and other system errors as part of the noise, and can be more reasonably used as a reference factor for adaptive modulation and coding.

The above researches aim at single user adaptive OFDM. Nowadays, OFDMA has become a hot research topic in the field of UWA communication. In terms of protocols, Bouabdallah and Boutaba [27] proposed a distributed OFDMA protocol, where each node optimizes its transmission power, subcarrier spacing and guard time duration by an adaptive allocation algorithm. Cheon and Cho [28] proposed a node-grouped OFDM medium-access-control protocol, where nodes are grouped by distances from the sink node, and then optimal sub-channel selection is carried out for each group. The above protocol layer research is limited to the design of the protocol, and does not consider the physical layer factors and system implementation. In terms of physical layer algorithms, Tu *et al.* [29] proposed a receiver processing algorithm based on a two-user OFDMA system, and can implement user-specific Doppler compensation by means of multiple resampling branches, where contiguous and interleaved carrier assignment schemes are compared. However, the above research is limited to the two-user fixed OFDMA scheme, which does not fully utilize the channel dynamic fading performance to maximize band utilization. Ma *et al.* [30] firstly combined superposition coding (SC) with OFDM modulation for UWA downlink communications, where the transmitter splits the power between two users based on statistical CSI. The expressions to characterize the boundary of the ergodic rate region achievable by the proposed scheme over long codewords are presented first, followed by the analysis of outage probability when coding is applied within one OFDM block. To sum up, based on the limitations of the above studies, it inspires us to use physical layer CSI for adaptive OFDMA research. The cross-layer design combined with channel feedback in physical layer and resource optimization in data link layer can make full use of UWA channel characteristics to maximize system spectrum utilization.

UWA adaptive technology distributes the limited network resources according to the CSI, and obtaining effective CSI is the premise. In the UWA adaptive OFDMA system, the CSI obtained at the transmitter is not perfect: due to the large propagation delay and the time-varying characteristic of the UWA channel, the CSI keeps changing during the feedback period. Especially in a multi-user network, it must go through multiple rounds of handshake to obtain CSI for each node. In addition, in order to avoid the collision of each node, the time interval between two packets is relatively large. The changes of the CSI during this period have a non-negligible impact on the UWA adaptive OFDMA system.

At present, some literatures have studied the resource allocation for adaptive OFDM/OFDMA system based on CSI. In [15], a heuristic resource allocation method for underwater uplink OFDMA system was proposed to reduce computational complexity, but it assumes that the channel state is unchanged during the time between channel measurement and resource allocation. In [19], the outdated CSI was used to predict the CSI at the time of data transmission, but it allows the time delay to be only one OFDM block length. In [23], outdated-average CSI is considered for channel feedback, and the performance based on outdated-average CSI is better than that by outdated-instantaneous CSI only for a part of users in the network, inversely worse for the other users. And the reason of the performance differences between the outdated-average CSI and the outdated-instantaneous CSI for resource allocation has not been discussed. Therefore, this paper detailedly analyses the outdated CSI and proposes an adaptive OFDMA system with low-overhead and limited feedback in time-varying UWA channel. A data fitting method is proposed for channel reconstruction, and compared with traditional group quantization methods [23]. Then we define the PSCTS and long-term statistical mean value as two indicators of outdated CSI for optimizing CSI feedback in UWA channel with large propa-

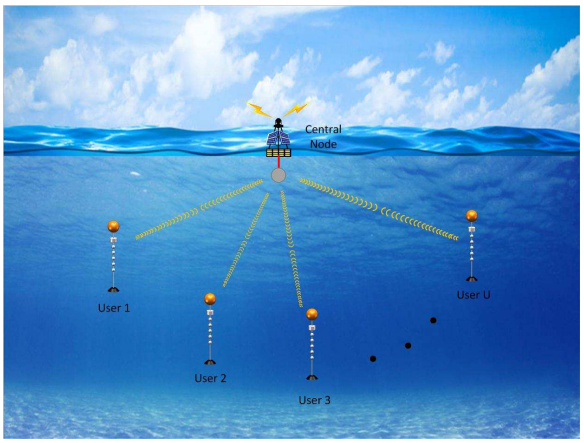

FIGURE 1. The temporal correlation coefficients in sea trial.

gation delay. Finally, a CSI selection method based on CCA factor is proposed, where CSI used for feedback is selected between outdated-instantaneous CSI and outdated-average CSI according to the CCA factor in the current observation period.

The remainder of this paper is organized as follows. Section II builds a practical OFDMA system, and gives a multiuser subcarrier and power allocation algorithm. Section III proposes a data fitting method for channel reconstruction, which is compared with the traditional group quantization method in simulations. Section IV defines two indicators of outdated-instantaneous CSI, including PSCTC factor and channel long-term statistics. Section V gives a CSI selection method between outdated-instantaneous CSI and outdated-average CSI. Section VI studies the system performance under the actual outdated CSI through the sea test. Section VII concludes this paper.

II. SYSTEM MODEL

A. OFDMA SETUP

Consider a UWA downlink scenario where one center node needs to send data to several distributed users, as shown in Fig. 1. Assume an OFDMA setup, where a total of K subcarriers are split into three sets: S_N of K_N null subcarriers to facilitate Doppler compensation at the receiver, S_P of K_P pilot subcarriers to assist channel estimation, and S_D of $K_D = K - K_N - K_P$ data subcarriers.

In each OFDMA block, the K_N null and K_P pilot subcarriers are shared by all the downlink U users, but the data subcarriers need to be allocated to serve different users.

Define the following variables.

$\delta[u,k]$: Subcarrier allocation factor, which indicates whether the kth carrier is assigned to the uth user, and a value of 1 means that the kth carrier is assigned to the uth user, otherwise, the value is 0.

$b[u,k]$: Bit loading factor, which means that the number of bits carried on the kth subcarrier for the uth user, and determines the modulation constellation.

$\beta[u,k]$: Power scaling factor, which determines the transmission power on the kth subcarrier for the uth user. If there is no variation in power scaling, $\beta[u,k] = 1$.

Assuming that the data subcarriers allocated to different users do not overlap, we have

$$\sum_{u=1}^{U} \delta[u,k] = 1. \tag{1}$$

The set of subcarriers for the uth user can be expressed as

$$\sum_{u=1}^{U} \sum_{k \in S_D} \delta[u,k] = K_D. \tag{2}$$

$$S_u = \{k | \delta[u,k] = 1, k \in S_D\}. \tag{3}$$

The data rate for the uth user can be expressed as

$$R_u = \sum_{k \in S_D} \delta[u,k] b[u,k] = \sum_{k \in S_u} b[u,k], \tag{4}$$

and the sum data rate of the UWA communication system is $R = \sum_{u=1}^{U} R_u$.

For each user, CSI on each data subcarrier can be estimated by pilots using the Orthogonal Matching Pursuit (OMP) algorithm in [31]. When multiple hydrophones are used for receiving, the equivalent input-output model after maximum ratio combining (MRC) can be written as follows [21]

$$z[u,k] = \hat{H}[u,k]\sqrt{\beta[u,k]}s[u,k] + \omega[u,k], \quad k \in S_u, \tag{5}$$

where $\hat{H}[u,k]$ is the estimated channel gain, $s[u,k]$ is the transmitted symbol, and $\omega[u,k]$ represents the error caused by ambient noise and channel estimation. CSI can be measured in the form of SNR, which can be expressed as

$$\hat{\gamma}[u,k] = \frac{\left|\hat{H}[u,k]\right|^2 \sigma_s^2}{\sigma_w^2[u]}, \tag{6}$$

where σ_s^2 is the symbol energy, $\sigma_w^2[u]$ is the noise variance of the uth user.

The total transmission power including a fixed amount of power spent on the pilot subcarriers and the total power spent on data subcarriers is

$$P_{total} = \sigma_s^2 \sum_{u=1}^{U} \sum_{k=1}^{K} \delta[u,k]\beta[u,k]. \tag{7}$$

B. RESOURCE ALLOCATION SCHEME

QAM modulation is adopted and BER can be approximately represented as [32]

$$BER[u,k] \approx 0.2 \exp\{-g(b[u,k])\beta[u,k]\hat{\gamma}[u,k]\}. \tag{8}$$

The constellation mapping factor $g(.)$ in the form can be written as [32]

$$g(b) = \begin{cases} \dfrac{6}{5 \times 2^b - 4}, & b = 1, 3, 5 \ldots \\ \dfrac{6}{4 \times 2^b - 4}, & b = 2, 4, 6 \ldots. \end{cases} \tag{9}$$

The process of the resource allocation algorithm is described as follows

1) PARAMETERS INITIALIZATION

The initial subcarrier allocation factor $\delta\,[u,k]$, the bit loading factor $b[u,k]$, the initial data rate R_u and the initial power consumption $P[u,k]$ for all users are set to 0. The sum rate $\sum_u R_u$ is set to be a target data rate R_{target}, and the BER $\mathcal{P}_E$ is set to be a target value $\mathcal{P}_{target}$. The power consumption of loading m bits to the corresponding subcarrier is as follows

$$P[u,k] = -\ln(5P_E)/[g(m)\hat{\gamma}[u,k]]. \tag{10}$$

2) SUBCARRIER ALLOCATION

All U users are polled to select the subcarrier which costs the lowest power for loading m bits until all carriers are selected.

The uth user checks the list of available subcarriers that not selected by other nodes, and finds the $\hat{k}_c$th subcarrier with the least power consumption when the additional m information bits are loaded.

$$\hat{k}_c = \arg\min_k P[u,k]. \tag{11}$$

The uth user selects subcarrier, and sets subcarrier allocation factor to 1

$$\delta[u,\hat{k}_c] = 1. \tag{12}$$

If the uth user first loads bits to the $\hat{k}$th subcarrier, which means the $\hat{k}$th subcarrier is allocated to the uth user, and other users cannot take up the $\hat{k}$th subcarrier again, and mark the subcarrier allocation factor as

$$\delta[u',\hat{k}] = 0 \quad u' \neq u. \tag{13}$$

3) POWER ALLOCATION

After all subcarriers are allocated, the power scaling factor of each subcarrier is calculated

$$\beta[u,k] = \frac{\delta[u,k]P[u,k]}{\sum_u \sum_k \delta[u,k]P[u,k]} K_D. \tag{14}$$

So we can get the optimal value $\delta[u,k]$ of and $\beta[u,k]$.

III. CSI RECONSTRUCTION

In this paper, we propose the data fitting algorithm as a new method for CSI reconstruction, and compare with the traditional group quantization method for CSI reconstruction, so as to provide efficient and reliable candidate solutions for CSI reconstruction.

A. DATA FITTING METHOD FOR CSI RECONSTRUCTION

In data processing, for the known variable x and its function value y, its features can use (15) as an approximate expression of the unknown function

$$y = f(x, a_1, a_2, \ldots, a_n), \tag{15}$$

where $a_1, a_2, \ldots, a_n$ are the undetermined constants. The $n-1$ polynomial fitting formula of the point pair (x_i, y_i) is

$$y = a_n x^{n-1} + a_{n-1}x^{n-2} + \ldots + a_2 x + a_1 + \varepsilon, \tag{16}$$

where ε is a random error that follows a normal distribution.

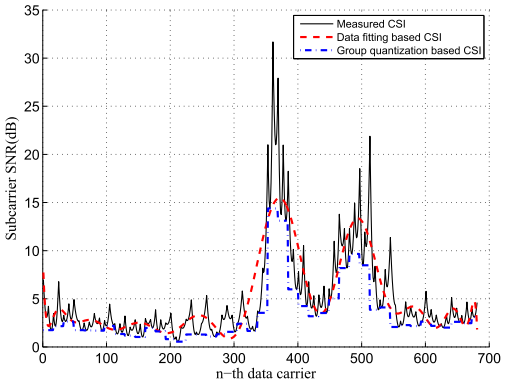

FIGURE 2. Data fitting vs. group quantization methods for reconstructing the measured CSI.

The data fitting process includes two steps: obtaining the function y and finding the fitting value a_n according to the y.

Therefore, we only need to take the CSI γ as the function value y to get the polynomial

$$\gamma = a_n x^{n-1} + a_{n-1}x^{n-2} + \ldots + a_2 x + a_1 + \varepsilon. \tag{17}$$

Then we select the appropriate fitting order to reconstruct the CSI. For example, assuming that we set the fitting order to 5, where the reconstructed CSI can be expressed as

$$\hat{\gamma} = a_6 x^5 + a_5 x^4 + a_3 x^2 + a_2 x + a_1. \tag{18}$$

Therefore, we only need to transmit 6 polynomial constants $a_1, a_2, a_3, a_4, a_5, a_6$, and the feedback overhead is greatly reduced.

B. DATA FITTING VS. GROUP QUANTIZATION METHODS

In this section, we fit the CSI obtained from sea test in South China Sea on May 8, 2014, and compared with the traditional group quantization method for CSI reconstruction. The subcarrier SNR measured at the receiver is denoted as the measured CSI, which has a big fluctuation and is shown by the solid curve in Fig. 2. Every 16 subcarriers will be combined into one group, and the group SNR is defined as the minimum subcarrier SNR of the 16 subcarriers, which is shown by the dotted curve in Fig. 2. Data fitting method with a fitting order of 5 is used for reconstructing the measured CSI, which is shown by the dotted curve in Fig. 2.

Observing from Fig.2, we can find 1) the fitting has a smooth effect on channel glitches; 2) the trend of the data fitting curve is consistent with the group quantization curve; 3) data fitting can well retain the changing trend of frequency-selective fading channel.

Then we analyze the influence of data fitting order on the MSE between the data fitting based CSI and the measured CSI. Observing from Fig.3, we can see that the higher the order, the lower the MSE. However, with the increase of order, the decrease of MSE is not obvious, so we should choose the appropriate order to fit the CSI.

In simulations, the stochastic UWA channel model uses $N_p = 15$ discrete paths, with the inter-arrival times

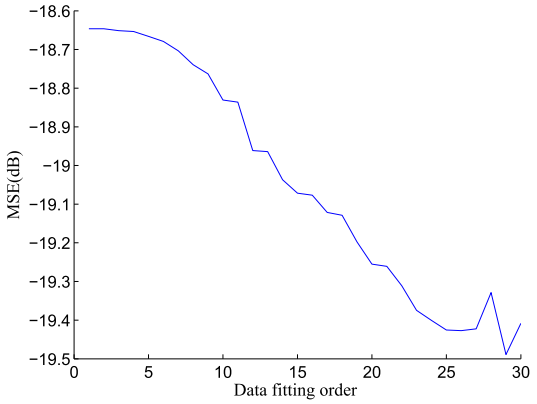

FIGURE 3. MSE between the data fitting based CSI and measured CSI.

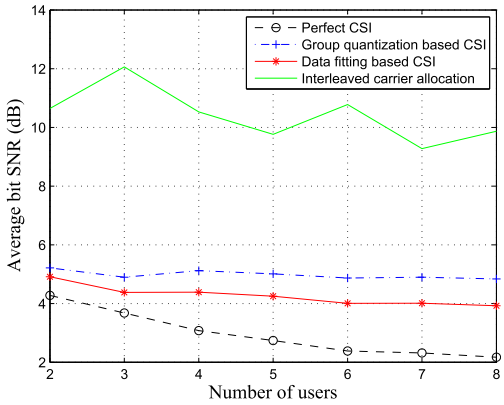

FIGURE 4. Average bit SNR with different CSI reconstruction scheme.

distributed exponentially with mean $E[\tau_{p+1} - \tau_p] = 1$ ms. Hence, the average channel delay spread is about 15 ms. The amplitudes are Rayleigh distributed with the average power decreasing exponentially with delay, where the difference between the beginning and the end of the guard time of 24.6 ms is 20 dB [31]. The resource allocation scheme is proposed in section II B.

Each OFDM block contains 512 data subcarriers, and we choose a uniform quantization with 16 quantization levels for both group-quantization method and data fitting method. For group-quantization method, every 16 subcarriers are combined into one cluster, resulting 32 clusters to cover 512 subcarriers for CSI feedback. Each users feedback message contains one data block of 18 bytes, one byte for the minimum SNR, one byte for the step size in the quantization, and 16 bytes of quantization outputs for 32 clusters. For data fitting method, we set the fitting order to 5 with 6 fitting factors, and there are 5 bytes in total for data fitting based CSI. So in this case, the feedback overhead by data fitting method is nearly 1/4 of group quantization method.

Given the total data rate and the BER requirements, we aim to optimize the power consumption of the system. In this paper, the average bit SNR is used to measure the average power consumption to send one bit, and defined as the ratio of the average bit transmission power P_{bit} to the noise power spectrum density N_0

$$averagebitSNR = \frac{P_{bit}}{N_0}, \tag{19}$$

where the average bit transmission power P_{bit} is defined as the ratio of the total transmission power P_{total} to the total number of transmitted bits b_{total}

$$P_{bit} = \frac{P_{total}}{b_{total}}. \tag{20}$$

Because the total number of transmitted bits b_{total} and the power spectrum density N_0 are constant, so the total transmission power is directly proportional to the average bit SNR.

We analyze the average bit SNR of resource allocation by using data fitting based CSI and group quantization based CSI. Resource allocation by using perfect CSI and interlaced carrier allocation are used as reference. The adaptive allocation algorithm is proposed in section 3.2. From Fig. 4 we can see:

1. All adaptive resource allocation schemes have much lower power consumption and are more robust than interleaving carrier allocation.

2. Resource allocation by using perfect CSI has the lowest power consumption.

3. Resource allocation by using data fitting based CSI has lower power consumption than that of group quantization based CSI.

4. Average power consumption decreases as the number of users increase in adaptive resource allocation.

Then we analyze the effective throughput of resource allocation by using data fitting based CSI and group quantization based CSI. The effective throughput is defined as: the amount of valid data successfully sent in a unit of time.

In the proposed UWA OFDMA system, control messages are accessed at fixed time slot. In a data transmission period, set the period of RTS, CTS, DATA, and Test signals to 5s respectively, which leads one communication cycle to 20s. The information is sent in the form of data packet, and one packet contains 20 OFDM blocks, where the sum rate of each block is 1024 bits. In the ideal case, the maximum effective throughput is 1024 bps.

When the user number changes, we can find the following conclusions from Fig. 5,

1. The effective throughput of adaptive resource allocation is larger than that of interleaved carrier allocation.

2. Resource allocation by using perfect CSI has the maximum effective throughput, and the effective throughput of resource allocation by using data fitting based CSI is more than that of group quantization based CSI.

3. For any adaptive resource allocation scheme, we can see that the effective throughput increases as the user number increases, and resource allocation by using perfect CSI increases the most.

From Fig. 6, we can see that the relative performance of several resource allocation schemes is basically

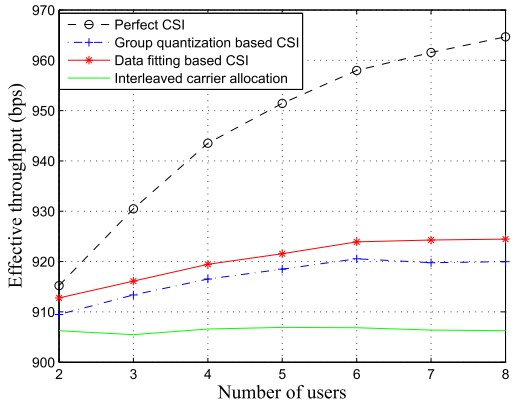

FIGURE 5. Effective throughput with different CSI reconstruction scheme (different user number).

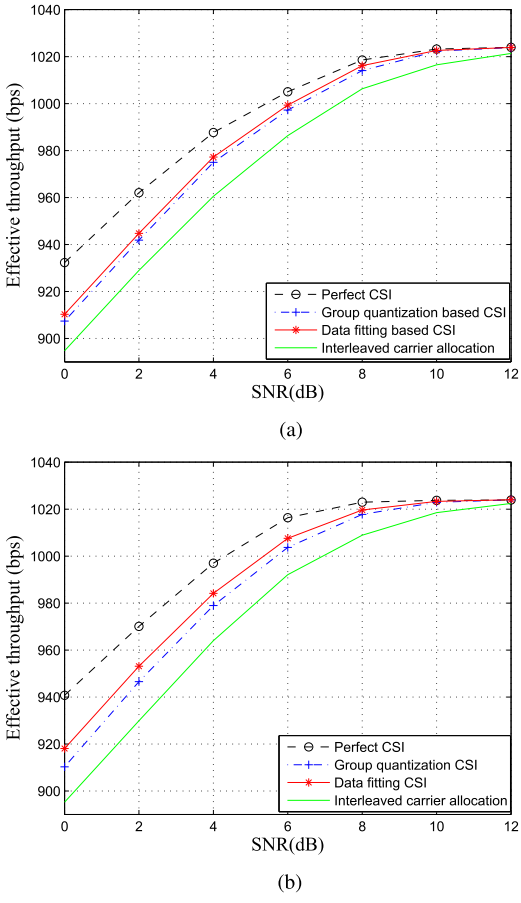

FIGURE 6. Effective throughput with different CSI reconstruction scheme (different SNR). (a) Two-user system. (b) Four-user system.

consistent with Fig. 5. With the increase of the SNR, the effective throughput of the adaptive system is improved and is approaching to the limit. Therefore, in the system design, the SNR and effective throughput can be compromised, and the effective throughput can be guaranteed without excessively increasing the transmission power.

As presented by [33, (14), (20)–(22)], the theoretical BER of each data carrier can be calculated with corresponding SNRs. Averaging all the data carriers, we can obtain the

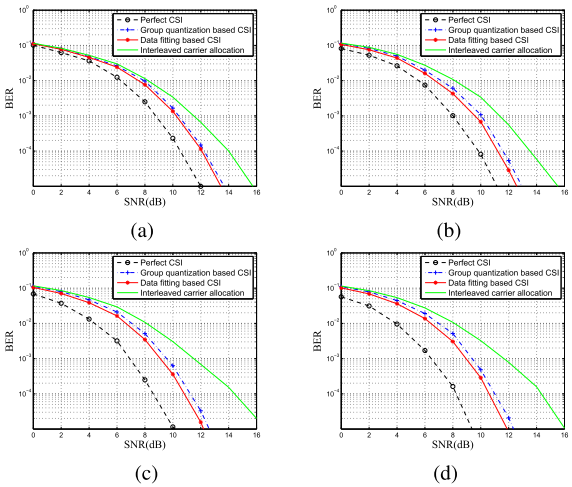

FIGURE 7. BER with different CSI reconstruction scheme. (a) Two-user system. (b) Four-user system. (c) Six-user system. (d) Eight-user system.

theoretical BER. Fig.7 shows the BER vs SNR curves for a two-user system, a four-user system, a six-user system and an eight-user system respectively. At a BER level of 10^{-3}, from all multi-systems, we can see that the interleave carrier allocation scheme has the worst performance, and the allocation scheme with perfect CSI performs the best. For the remaining two allocations schemes, the resource allocation by using data fitting based CSI performs better than that of group quantization based CSI. As the number of users increase, the BER of resource allocation scheme is getting lower and lower, but the BER of interleaved carrier allocation scheme is almost unchanged. This is because the adaptive resource allocation scheme can select the subcarriers with higher SNR for a certain user, and balance the subcarrier allocation for all users. As the number of user increases, each user can select more suitable subcarriers.

Therefore, data fitting is an effective candidate for CSI reconstruction. A certain fitting algorithm can not only be applied to all kinds of channels, which is not limited to channel conditions and amount of the CSI, but also cost less feedback overhead than traditional group quantization method. So we use data fitting for CSI reconstruction and data analysis in the experiment.

IV. CSI INDICATED

A. PER-SUBCARRIER CHANNEL TEMPORAL CORRELATION (PSCTC)

To better understand the impact of the delay on the quality of channel feedback, the PSCTC coefficient ρ on the kth data subcarrier over different time series $\mathbf{n}_1$ and $\mathbf{n}_2$ is computed as (21), as shown at the bottom of the next page where $\hat{\gamma}[n_p, k]$ is the signal-to-noise ratio (SNR) on kth data subcarrier from the first packet to the nth packet over time series $\mathbf{n}$. ρ=1 represents complete correlation, ρ=0 represents unrelated.

As shown in Fig.8, for example, when $\mathbf{n}_1$ is the time sequence of receiving RTS, and $\mathbf{n}_2$ is the time sequence of the

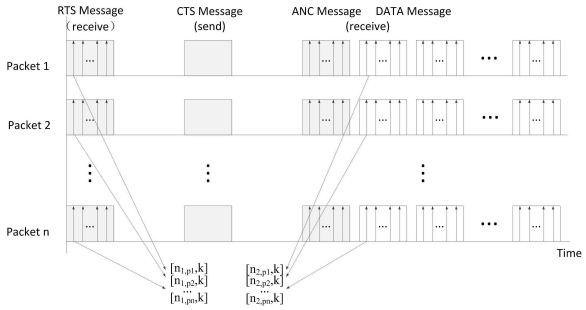

FIGURE 8. Subcarrier correlation coefficient diagram.

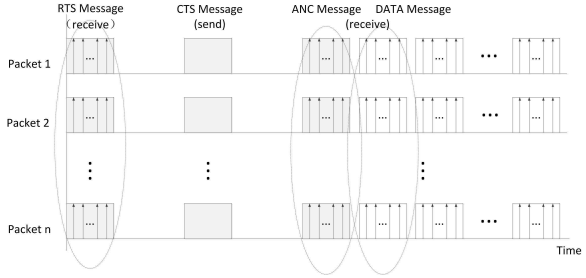

FIGURE 9. UWA OFDMA handshake time statistical sample.

start of the data burst, the calculated correlation coefficient is the correlation between CSI estimation time and actual data starting time.

B. LONG-TERM CHANNEL STATISTICS

Because the propagation delay is large in UWA system, so the feedback CSI could be completely outdated. In such a case, we choose long-term channel statistics as a CSI standard, for example, suppose $\hat{\gamma}[n,k]$ follows an exponential distribution with the mean of $\bar{\gamma}[n,k]$, then we use $\bar{\gamma}[n,k]$ to represent CSI.

According to (8), the average BER can be written as

$$\begin{aligned}\overline{BER}[u,k] &\approx E\{0.2\exp\{-g(b[u,k])\beta[u,k]\hat{\gamma}[u,k]\}\} \\ &= \frac{0.2}{1+g(b[u,k])\beta[u,k]\bar{\gamma}[u,k]}. \end{aligned} \tag{22}$$

The same allocation algorithm can be applied for it, with (10) updated as

$$P[u,\hat{k}] = -\frac{1-5P_E}{5P_E\bar{\gamma}[u,k]g(b[m])}. \tag{23}$$

The circles in Fig.9 show the calculation of different CSI respectively: the average CSI of the request-to-send(RTS) message, the announcement(ANC) message, and the start of the data burst is calculated by long-term channel statistics from the first packet to the nth packet.

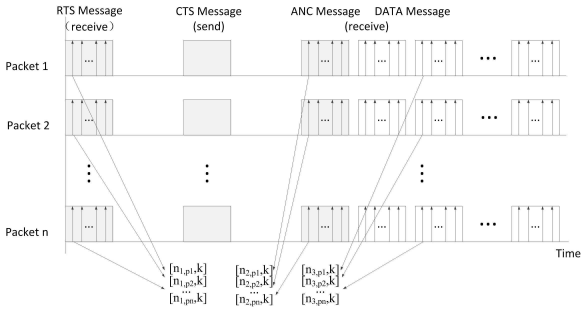

FIGURE 10. CCA factor diagram.

V. CCA METHOD TO SELECT BETWEEN OUTDATED-INSTANTANEOUS CSI AND OUTDATED-AVERAGE CSI

A. CCA METHOD

From section 4.2 we can select outdated-average CSI as feedback CSI, but sometimes its performance is not necessarily better than that of outdated-instantaneous CSI [34]. So this section will discuss how to select between the outdated-instantaneous CSI and outdated-average CSI for resource allocation. In this section, we use data fitting method to reconstruct CSI, and the time-vary UWA channel model is proposed in [35], we adjust the channel time-varying by changing some parameters such as time-varying Doppler scaling factor, which is related to the speed and angle of receiver.

We define the CCA factor as the attenuation of PSCTC coefficients over a given period of time. As shown in Fig. 10, the CCA factor on the kth data subcarrier over different time series $\mathbf{n}_1$ and $\mathbf{n}_2$ is computed by taking time series $\mathbf{n}_3$ as the observation value (24), as shown at the bottom of the next page.

When the given period of time is invariable, the larger the CCA factor is, the faster the channel changes. Assuming that time series $\mathbf{n}_2$ coincides with $\mathbf{n}_3$, CCA factor is computed as (25), as shown at the bottom of the next page.

Fig.11 shows the change of CCA factor over time delay. We can see the CCA factor increases as the delay increases. In the first 3 seconds, the CCA factor increased obviously, and after 5 seconds, the change of CCA factor is stable. And the CCA factor of outdated-average CSI is smoother than that of outdated-instantaneous CSI. We find that when channel change fast, the CCA factor of outdated-instantaneous CSI becomes lower than that of outdated-average CSI, because outdated-average CSI will use the long time statistics of the channel, which includes lots of outdated-instantaneous CSI.

We calculated the CCA factor in three seconds, which means the interval between time series $\mathbf{n}_1$ and $\mathbf{n}_2$ is

$$\rho[k;p_n;n_1,n_2] = \frac{E\{(\hat{\gamma}[n_{1,p_n},k]-E[\hat{\gamma}[n_{1,p_n},k]])(\hat{\gamma}[n_{2,p_n},k]-E[\hat{\gamma}[n_{2,p_n},k]])\}}{\sqrt{var(\hat{\gamma}[n_{1,p_n},k])var(\hat{\gamma}[n_{2,p_n},k])}}, \tag{21}$$

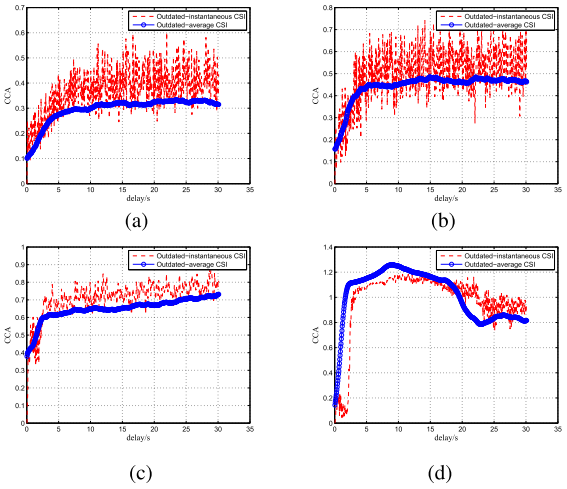

FIGURE 11. CCA over time delay. (a) Node A(RX vehicular speed=0 RX vehicular angle=0). (b) Node B(RX vehicular speed=5 RX vehicular angle=0). (c) Node C(RX vehicular speed=5 RX vehicular angle=0.2). (d) Node D(RX vehicular speed=5 RX vehicular angle=0.5).

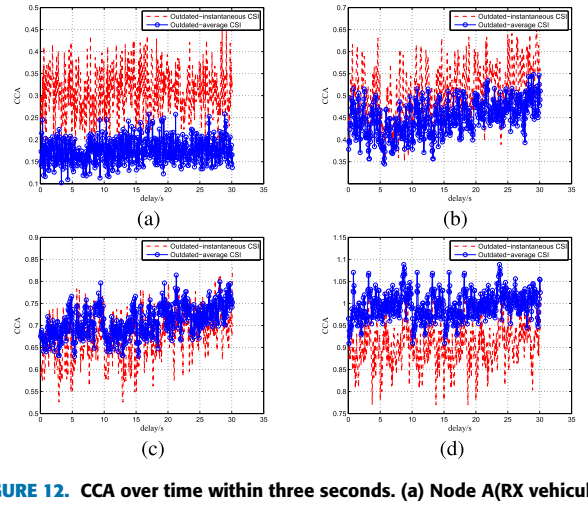

FIGURE 12. CCA over time within three seconds. (a) Node A(RX vehicular speed=0 RX vehicular angle=0). (b) Node B(RX vehicular speed=5 RX vehicular angle=0). (c) Node C(RX vehicular speed=5 RX vehicular angle=0.2). (d) Node D(RX vehicular speed=5 RX vehicular angle=0.5).

three seconds. From Fig.12 we can see the change of CCA factor is relatively stable, and the variation range of CCA factor is between 0 and 0.2. From Fig.12(a) and Fig.12(d) we can see, when the CCA factor of outdated-instantaneous CSI is smaller than 0.4, the CCA factor of outdated-average CSI is lower than that of outdated-instantaneous CSI, but when the CCA factor of outdated-instantaneous CSI is larger than 0.8, the opposite is true. From Fig.12(b) and Fig.12(c) we can see, when the CCA factor of outdated-instantaneous CSI is between 0.4 and 0.8, the CCA factor of these two kinds of CSI are close to each other.

Therefore, we set the CCA factor of outdated-instantaneous CSI to 0.6 as the threshold to select suitable CSI for feedback. According to(26), if the CCA factor is higher than 0.6, we select outdated-instantaneous CSI for feedback, conversely, we select outdated-average CSI for feedback. We call it CSI selection based on CCA method.

$$CSI_{feedback} = \begin{cases} outdated - instantaneous\ CSI & CCA > 0.6 \\ outdated - average\ CSI & CCA \leq 0.6. \end{cases} \quad (26)$$

B. OFDMA HANDSHAKING MODEL BASD ON CCA METHOD

In the proposed channel adaptive OFDMA system, the control information exchange adopts fixed time-sequence access, and the subcarrier orthogonality is used to implement multi-node conflict-free data transmission. In the experiment, the CSI feedback is obtained through the control information by handshake, and the resource allocation scheme is obtained through the adaptive allocation algorithm. And the multi-node information is processed off-line according to the allocation scheme and record. We consider a handshaking process of adaptive OFDMA as shown in Fig. 13.

Each receiving node estimates the outdated-instantaneous CSI based on the request-to-send (RTS) message, the previous CSIs will be used to calculate the outdated-average CSI. Test message used to calculate the CCA factor with RTS message, each node selects between the outdated-instantaneous CSI and outdated-average CSI according to the CCA factor, and the CSI is embedded in the clear-to-send (CTS) messages. The central node collects the CSIs of all the receiving nodes, and runs an algorithm to obtain a subcarrier allocation solution. At last, the central node broadcasts the allocation

$$\begin{aligned} \Delta\rho[k; p_n; n_1, n_2|n_3] &= \rho[k; p_n; n_2, n_3] - \rho[k; p_n; n_1, n_3] \\ &= \frac{E\{(\hat{\gamma}[n_{2,p_n}, k] - E[\hat{\gamma}[n_{2,p_n}, k]])(\hat{\gamma}[n_{3,p_n}, k] - E[\hat{\gamma}[n_{3,p_n}, k]])\}}{\sqrt{var(\hat{\gamma}[n_{2,p_n}, k])var(\hat{\gamma}[n_{3,p_n}, k])}} \\ &\quad - \frac{E\{(\hat{\gamma}[n_{1,p_n}, k] - E[\hat{\gamma}[n_{1,p_n}, k]])(\hat{\gamma}[n_{3,p_n}, k] - E[\hat{\gamma}[n_{3,p_n}, k]])\}}{\sqrt{var(\hat{\gamma}[n_{1,p_n}, k])var(\hat{\gamma}[n_{3,p_n}, k])}}, \end{aligned} \quad (24)$$

$$\begin{aligned} \Delta\rho[k; p_n; n_1, n_2|n_2] &= \rho[k; p_n; n_2, n_2] - \rho[k; p_n; n_1, n_2] \\ &= 1 - \frac{E\{(\hat{\gamma}[n_{1,p_n}, k] - E[\hat{\gamma}[n_{1,p_n}, k]])(\hat{\gamma}[n_{2,p_n}, k] - E[\hat{\gamma}[n_{2,p_n}, k]])\}}{\sqrt{var(\hat{\gamma}[n_{1,p_n}, k])var(\hat{\gamma}[n_{2,p_n}, k])}}, \end{aligned} \quad (25)$$

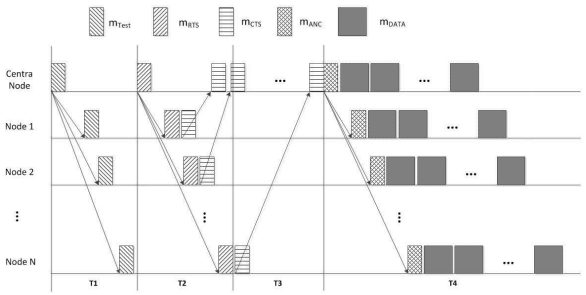

FIGURE 13. Handshaking process of adaptive OFDMA.

table and data packets to all the users, in which the allocation table is included in an announcement (ANC) message in front of the data packets. Each receiving node demodulates its own data based on the allocation solution from the central node. In particular, if the interval between two packets is short, we can use the CSI estimated by the previous packet instead of the CSI estimated by the test signal.

The CSI carried by CTS message is the CSI estimated by RTS message at time T2, so when the central node allocates resources to each nodes according to the CSI carried by CTS message and broadcasts signals at time T4, the CSI in the current RTS message is outdated under time-varying UWA channel.

C. SIMULATION RESULTS OF CCA METHOD

Fig. 14 shows BER performance with four kinds of feedback CSI: current CSI, outdated-instantaneous CSI(RTS), outdated-average CSI and the CSI selected according to CCA method, and interleaved carrier allocation scheme is to be a reference. Fig.14(a) is two-user system with node A and node D, and Fig.14(b) is four-user system with all nodes. We can see the BER performance of adaptive resource allocation scheme is better than that of interleaved carrier allocation, and resource allocation by using current CSI has the best performance. In the two-user system, resource allocation by using outdated-instantaneous CSI(RTS) is better than that of outdated-average CSI, but in the four-user system, resource allocation by using outdated-instantaneous CSI(RTS) is little worse than that of outdated-average CSI. The performance of CCA method is always better than that of only use one kind CSI for feedback.

VI. EXPERIMENTAL RESULTS

A. TEST PARAMETERS

We carried out sea trial in South China Sea on May. 8, 2014. In the experiment, two ships are used for communication. One ship is anchored as the central node, and the four-element line array in the ship is used for receiving the experimental signal, and another ship is used as the subnodes to transmit the experimental signal at different distances (from 1km to 5km). The transmission interval of each experimental signal is 2.2 seconds. The frame structure of the experimental signal is as shown in Fig. 15, one frame experimental signal lasts

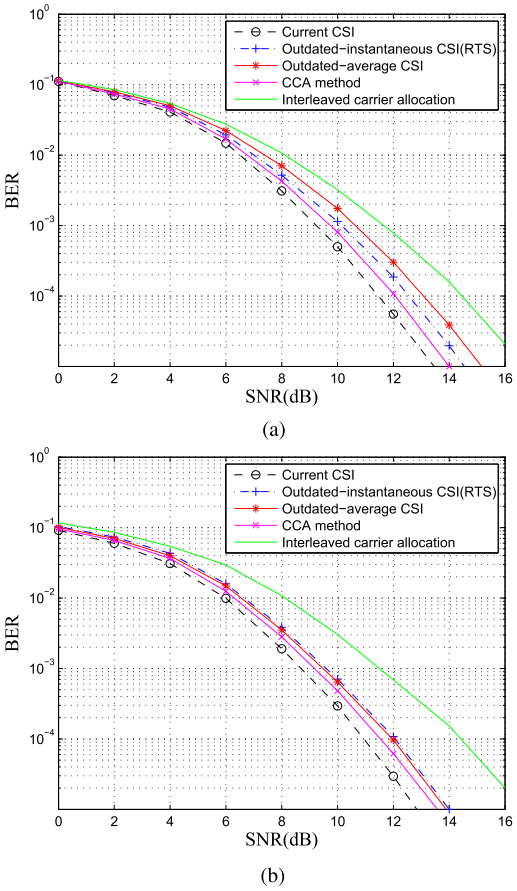

FIGURE 14. BER with different allocation scheme. (a) Two-user system. (b) Four-user system.

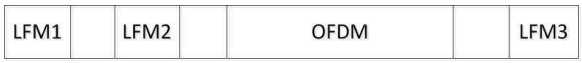

FIGURE 15. The frame structure of the test signal.

for 1.8 seconds, which contains three LFM(Linear Frequency Modulation) signals and eight OFDM blocks. LFM1 signal is used for signal synchronization, LFM2 signal and LFM3 signal are the same signal, which are used for Doppler estimation. All CSIs are estimated from LFM1 and LFM3. One OFDM block has 681 subcarriers, which contains 595 data subcarriers and 86 pilot subcarriers, and the pilot interval is 8. Then we select four different experimental signals as test message, RTS message, CTS message and data message.

We can use different array elements at different distances to simulate different users in the network, which are divided into one central node O and four subnodes A, B, C and D. The transmission distances from the node O, nodes A, B, C and D are 1.1km, 1.3 km, 2.2km and 3.5 km, respectively.

B. CSI RECONSTRUCTION RESULTS

We choose two nodes, three nodes and four nodes as two-user system three user- system, and four-user system respectively. A rate-1/2 64-state convolution code is introduced during

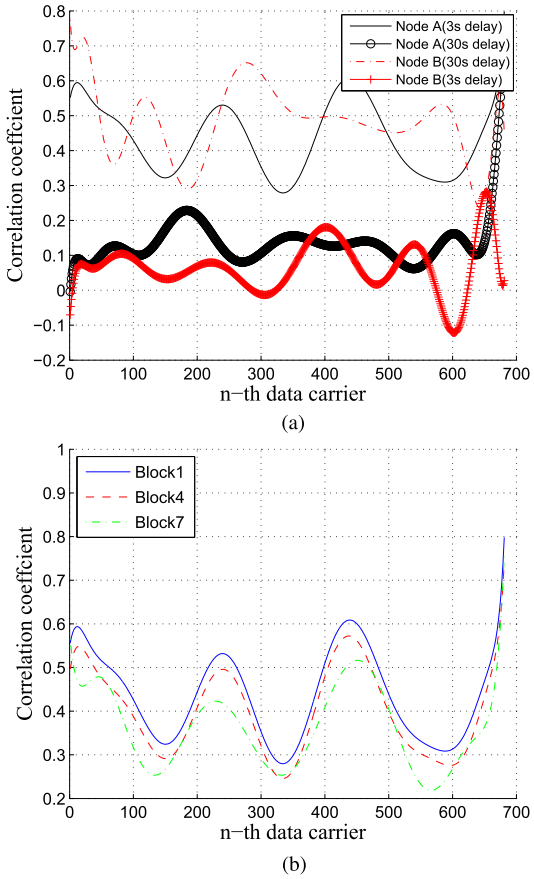

FIGURE 16. Per-subcarrier channel temporal correlation in OFDMA. (a) different frame. (b) different block.

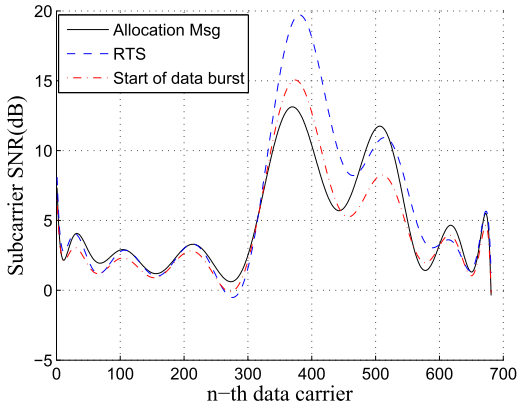

FIGURE 17. Per-subcarrier channel temporal correlation in OFDMA.

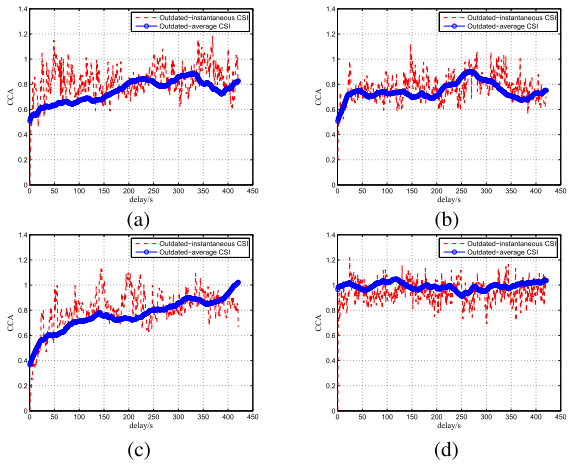

FIGURE 18. CCA over time delay. (a) Node A. (b) Node B. (c) Node C. (d) Node D.

off-line processing to expand the gaps among different results. Assume that an all-zero codeword needs to be transmitted, the coding matrix can be obtained as the decoding basis. The BER is directly compared with the all-zero transmitted signals.Table I shows the BER of multi-user system using different CSI reconfiguration scheme for resource allocation. We can see the resource allocation by using perfect CSI always shows the best performance. The performance on resource allocation by using date fitting based CSI is better than that of group quantization based CSI.

C. ANALYSIS BASED ON TIME-VARYING CHANNEL

We choose two sets of three test signals from node A and node B as RTS message, ANC message and the start of the data burst respectively. Fig. 16(a) shows the PSCTC coefficients on all the data subcarriers between the RTS message and the start of the data burst (30 seconds delay), and those between the ANC message and the start of the data burst (3 seconds delay). Obviously, the channel correlation of 3 seconds delay is much better than that of 30 seconds delay.

In Fig.16(b), the PSCTC coefficients between the first, fourth, seventh OFDM block of data packet and the ANC are given. The time intervals are 4.3s, 5.5s, and 6.8s, respectively. Firstly, the PSCTC coefficients between data subcarriers and ANC are mostly consistent in different symbol time. Secondly, as the time interval between two OFDM blocks increases, the correlation between the symbol and the ANC is slightly lower. As seen in Fig.16, in a certain time (a frame), the trend of the PSCTC coefficient is constant, and the channel correlation decreases with the increase of time delay.

Based on the study of the correlation of channel feedback information at different time, the relationship between the channel correlation and the time delay is inversely proportional under the UWA channel. And, the channel can show strong correlation only within a few seconds; even within a data packet, the increase of time interval also reduces the channel correlation.

As shown in Fig. 17, the average values of the subcarrier SNRs from RTS, allocation message, and start of data burst on each data subcarrier are obtained by averaging over multiple data sets.

D. CCA METHODS RESULTS

Fig.18 shows the change of CCA factor of four nodes. Fig.19 shows the trend of CCA factor within three seconds

TABLE 1. BER of multi-user system.

CSI reconfiguration scheme	undecoded			decoded		
	two-user system	three-user system	four-user system	two-user system	three-user system	four-user system
Data fitting based CSI	0.0357	0.0259	0.0161	$1.10e10^{-3}$	0	0
group quantization based CSI	0.0379	0.0282	0.0198	$1.40e10^{-3}$	$1.50e10^{-4}$	0
perfect CSI	0.0264	0.0178	$7.45e10^{-3}$	0	0	0

TABLE 2. BER of multi-user system.

CSI feedback scheme	undecoded			decoded		
	two-user system	three-user system	four-user system	two-user system	three-user system	four-user system
Interlaced carrier allocation	0.0538	0.0542	0.0556	$1.70e10^{-3}$	$1.80e10^{-3}$	$1.80e10^{-3}$
Outdated-instantaneous(RTS)	0.0498	0.0421	0.0229	$1.50e10^{-3}$	$1.40e10^{-3}$	$1.50e10^{-4}$
Outdated-average CSI	0.0431	0.0379	0.0248	$1.40e10^{-3}$	$1.00e10^{-3}$	0
CCA method	0.0408	0.0329	0.0184	$1.20e10^{-3}$	$1.50e10^{-4}$	0
Current CSI	0.0357	0.0259	0.0161	$1.00e10^{-3}$	0	0

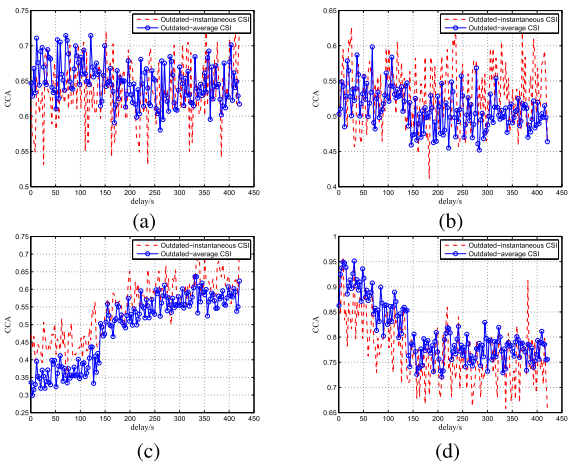

FIGURE 19. CCA over time within three seconds. (a) Node A. (b) Node B. (c) Node C. (d) Node D.

of four nodes. We can see that the result is basically the same as that of simulation in section V A. From Fig. 18 we can see that the CCA factor increases as the delay increases, and rose rapidly in a short period of time. Combined with Fig.18 and Fig.19, it can be seen that the channel of node D changes fastest, and the channel of node B and node C change slower. The channel time-varying trend of node A and node B is more stable than that of node C and node D. The channel of node C changes from slow to fast, and the channel of node D changes from fast to slow. When the CCA factor of outdated-instantaneous CSI is smaller than 0.4, the CCA factor of outdated-average CSI is lower than that of outdated-instantaneous CSI, but when the CCA factor of outdated-instantaneous CSI is larger than 0.8, the opposite is true. The CCA factor of these two kinds of CSI are close to each other when the CCA factor of outdated-instantaneous CSI is between 0.4 and 0.8. The CCA factors of all users change within the scope of 0.2 in three seconds.

Then we choose node A and node C as two-user system, node A, node B and node C as three user- system, all nodes as four-user system respectively.

Table 2 shows the BER of multi-user system using different CSI feedback scheme for resource allocation, and we use date fitting based CSI for feedback. The BER performance of adaptive resource allocation scheme is better than that of interleaved carrier allocation and resource allocation by using current CSI has the best performance. The performance based on CCA method is better than that of outdated-instantaneous CSI(RTS) and outdated-average CSI for all multi-user systems.

VII. CONCLUSION

In this paper, we study the performance of adaptive OFDMA under the outdated CSI in time-varying UWA channel, especially we study the time delay in CSI feedback and

its influence on system performance. Through the measured data, we can see that two kinds of limited feedback methods, subcarrier group quantization and data fitting, can effectively feedback information, and data fitting technology has better performance and lower overhead. Through the analysis of the outdated CSI, we can see that the correlation between subcarriers is inversely proportional to the time delay. The CSI is stable in a long time, which is a more robust form of channel feedback information. And we selected a specific CCA factor as the threshold to choose outdated-instantaneous CSI or outdated-average CSI for resource allocation, simulation and experimental results show that its performance has improved.

REFERENCES

[1] I. Kim, I.-S. Park, and Y. H. Lee, "Use of linear programming for dynamic subcarrier and bit allocation in multiuser OFDM," *IEEE Trans. Veh. Technol.*, vol. 55, no. 4, pp. 1195–1207, Jul. 2006.
[2] Y. F. Chen and J. W. Chen, "A fast subcarrier, bit, and power allocation algorithm for multiuser OFDM-based systems," *IEEE Trans. Veh. Technol.*, vol. 57, no. 2, pp. 873–881, Mar. 2008.
[3] S. Chieochan and E. Hossain, "Adaptive radio resource allocation in OFDMA systems: A survey of the state-of-the-art approaches," *Wireless Commun. Mobile Comput.*, vol. 9, no. 4, pp. 513–527, Apr. 2009.
[4] H. N. Vu and H.-Y. Kong, "Joint subcarrier matching and power allocation in OFDM two-way relay systems," *J. Commun. Netw.*, vol. 14, no. 3, pp. 257–266, Jun. 2012.
[5] W.-C. Pao, Y.-F. Chen, and M.-G. Tsai, "An adaptive allocation scheme in multiuser OFDM systems with time-varying channels," *IEEE Trans. Wireless Commun.*, vol. 13, no. 2, pp. 669–679, Feb. 2014.
[6] B. Li, S. Zhou, M. Stojanovic, L. Freitag, and P. Willett, "Multicarrier communication over underwater acoustic channels with nonuniform Doppler shifts," *IEEE J. Ocean. Eng.*, vol. 33, no. 2, pp. 198–209, Apr. 2008.
[7] Z. Wang, S. Zhou, J. Catipovic, and P. Willett, "Asynchronous multiuser reception for OFDM in underwater acoustic communications," *IEEE Trans. Wireless Commun.*, vol. 12, no. 3, pp. 1050–1061, Mar. 2013.
[8] Z. Liu and T. C. Yang, "On overhead reduction in time-reversed OFDM underwater acoustic communications," *IEEE J. Ocean. Eng.*, vol. 39, no. 4, pp. 788–800, Oct. 2014.
[9] Y. Chen, Z. Wang, L. Wan, H. Zhou, S. Zhou, and X. Xu, "OFDM-modulated dynamic coded cooperation in underwater acoustic channels," *IEEE J. Ocean. Eng.*, vol. 40, no. 1, pp. 159–168, Jan. 2015.
[10] A. Radosevic, R. Ahmed, T. Duman, J. Proakis, and M. Stojanovic, "Adaptive OFDM modulation for underwater acoustic communications: Design considerations and experimental results," *IEEE J. Ocean. Eng.*, vol. 39, no. 2, pp. 357–370, Apr. 2013.
[11] C. Wang, J. Yin, P. Du, and L. Guo, "Application of orthogonal frequency division multiplexing in cognitive underwater communication," *J. Acoust. Soc. Amer.*, vol. 132, no. 3, p. 2015, 2012.
[12] Y. Zhang, C. Wang, J. Yin, and X. Sheng, "Research on multilevel differential amplitude and phase-shift keying in convolution-coded orthogonal frequency division multiplexing underwater communication system," *J. Acoust. Soc. Amer.*, vol. 132, no. 3, p. 2015, 2012.
[13] J. Cheon, K. Son, S.-K. Lee, and H.-S. Cho, "An extension of node-grouped OFDMA MAC into multi-clustered networks," in *Proc. ACM Int. Conf. Underwater Netw. Syst.*, 2012, pp. 1–2.
[14] I. M. Khalil, Y. Gadallah, M. Hayajneh, and A. Khreishah, "An adaptive OFDMA-based MAC protocol for underwater acoustic wireless sensor networks," *Sensors*, vol. 12, no. 7, pp. 8782–8805, 2012.
[15] J. Cheon and H. S. Cho, "A heuristic resource allocation method for underwater uplink OFDMA system," in *Proc. 7th Int. Conf. Ubiquitous Future Netw.*, Jul. 2015, pp. 811–813.
[16] Y. Zhang, Y. Huang, and L. L. Wan, "Adaptive OFDMA for downlink underwater acoustic communications," in *Proc. IEEE Oceans*, 2015, pp. 1–5.
[17] J. Aparicio and T. Shimura, "OFDMA communication system for cooperative localization of underwater vehicles," in *Proc. IEEE Int. Workshop Signal Process. Adv. Wireless Commun.*, Jul. 2017, pp. 1–5.
[18] M. Stojanovic, "Adaptive channel estimation for underwater acoustic MIMO OFDM systems," in *Proc. Digit. Signal Process. Workshop, IEEE Signal Process. Educ. Workshop*, Jul. 2009, pp. 132–137.
[19] A. Radosevic, R. Ahmed, T. Duman, J. Proakis, and M. Stojanovic, "Adaptive OFDM modulation for underwater acoustic communications: Design considerations and experimental results," *IEEE J. Ocean. Eng.*, vol. 39, no. 2, pp. 357–370, Apr. 2013.
[20] L. Wan *et al.*, "Field tests of adaptive modulation and coding for underwater acoustic OFDM," in *Proc. 8th ACM Int. Conf. Underwater Netw. Syst.*, 2013, p. 35.
[21] L. Wan *et al.*, "Adaptive modulation and coding for underwater acoustic OFDM," *IEEE J. Ocean. Eng.*, vol. 40, no. 2, pp. 327–336, Apr. 2015.
[22] L. Ma, S. Z. Liu, and G. Qiao, "Sparse channel estimation and pilot optimization for underwater acoustic orthogonal frequency division multiple access uplink communications," *Acta Phys. Sinica*, vol. 64, no. 15, p. 154304, 2015.
[23] Y. Zhang, Y. Huang, L. Wan, S. Zhou, X. Shen, and H. Wang, "Adaptive OFDMA with partial CSI for downlink underwater acoustic communications," *J. Commun. Netw.*, vol. 18, no. 3, pp. 387–396, 2016.
[24] J. Rice and V. Mc Donald, "Adaptive modulation for undersea acoustic telemetry," *Sea. Technol.*, vol. 40, no. 5, pp. 29–36, May 1999.
[25] A. Benson, J. Proakis, and M. Stojanovic, "Towards robust adaptive acousitc communications," in *Proc. MTS/IEEE OCEANS*, Aug. 2000, pp. 1234–1249.
[26] S. Mani, "Adaptive modualtion technique for underwater acoustic channels," M.S. thesis, Dept. Elect. Eng., Arizona State Univ., Tempe, AZ, USA, Mar. 2008.
[27] F. Bouabdallah and R. Boutaba, "A distributed OFDMA medium access control for underwater acoustic sensors networks," in *Proc. IEEE Int. Conf. Commun. (ICC)*, Kyoto, Japan, Jun. 2011, pp. 1–5.
[28] J. Cheon and H.-S. Cho, "A delay-tolerant OFDMA-based MAC protocol for underwater acoustic sensor networks," in *Proc. IEEE Symp. Workshop Sci. Use Submarine Cables Related Technol. (SSC)*, Apr. 2011, pp. 1–4.
[29] K. Tu, T. Duman, and M. Stojanovic, "OFDMA for underwater acoustic communications," in *Proc. Commun., Control, Comput. (Allerton)*, Sep. 2011, pp. 633–638.
[30] L. Ma, S. Zhou, G. Qiao, S. Liu, and F. Zhou, "Superposition coding for downlink underwater acoustic OFDM," *IEEE J. Ocean. Eng.*, vol. 42, no. 1, pp. 175–187, Jan. 2017.
[31] C. R. Berger, S. Zhou, J. C. Preisig, and P. Willett, "Sparse channel estimation for multicarrier underwater acoustic communication: From subspace methods to compressed sensing," *IEEE Trans. Signal Process.*, vol. 58, no. 3, pp. 1708–1721, Mar. 2010.
[32] P. Xia, S. Zhou, and G. B. Giannakis, "Adaptive MIMO-OFDM based on partial channel state information," *IEEE Trans. Signal Process.*, vol. 52, no. 1, pp. 202–213, Jan. 2004.
[33] K. Cho and D. Yoon, "On the general BER expression of one-and two-dimensional amplitude modulations," *IEEE Trans. Commun.*, vol. 50, no. 7, pp. 1074–1080, Nov. 2002.
[34] G. Qiao, L. Lei, and L. Ma, "Analysis of outdated channel state information in underwater acoustic downlink OFDMA system," in *Proc. IEEE Oceans*, May 2018, pp. 1–5.
[35] P. Qarabaqi and M. Stojanovic, "Statistical characterization and computationally efficient modeling of a class of underwater acoustic communication channels," *IEEE J. Ocean. Eng.*, vol. 38, no. 4, pp. 701–717, Oct. 2013.

GANG QIAO received the B.S., M.S., and Ph.D. degrees from the College of Underwater Acoustic Engineering, Harbin Engineering University (HEU), China, in 1996, 1999, and 2004, respectively. Since 1999, he has been with the College of Underwater Acoustic Engineering, HEU, where he is currently a Professor and the Associate Dean. He has already published more than 80 papers and holds seven national invention patents. His current research interests include underwater communication and networks, detection and positioning of underwater targets, and the sonar designed for small carriers. He is a member of the Acoustical Society of China and the Youth Federation of Heilongjiang Province, and the Vice Chairman of the Robotics Society of Heilongjiang Province. He was a recipient of the National Award for the outstanding scientific and technological workers and the Science and Technology Award for Young Talents in Heilongjiang Province.

LEI LIU received the B.S. degree in underwater acoustic engineering from Harbin Engineering University, Harbin, China, in 2015, where he is currently pursuing the Ph.D. degree with the College of Underwater Acoustic Engineering. His current research interests include adaptive communication and communication networks for time-varying underwater acoustic channels.

LU MA received the B.S. and Ph.D. degrees in signal and information processing from Harbin Engineering University (HEU), Harbin, China, in 2010 and 2016, respectively. From 2014 to 2015, she visited the University of Connecticut, Storrs, CT, USA. From 2016 to 2018, she was an Assistant Professor with the College of Underwater Acoustic Engineering, HEU, where she is currently an Associate Professor. Her research interests lie in the areas of multicarrier and multiuser communications for underwater acoustic channels.

YANLING YIN received the B.S., M.S., and Ph.D. degrees from the College of Underwater Acoustic Engineering, Harbin Engineering University, China, in 2009, 2012, and 2016, respectively. Since 2016, she has been with the College of Electrical and Information, Northeast Agricultural University, China, where she is currently a Lecture. She has already published more than 14 papers and holds 15 national invention patents. Her current research interests include underwater acoustic communication and networks, deep learning, and machine learning.